Expression of the $\alpha_2\delta$ Subunit Interferes with Prepulse Facilitation in Cardiac L-type Calcium Channels

Daniela Platano,* Ning Qin,*# Francesca Noceti,* Lutz Birnbaumer,*‡§¶ Enrico Stefani,*†§ and Riccardo Olcese*
Departments of *Anesthesiology, †Physiology and ‡Biological Chemistry, and §Brain Research; ¶Molecular Biology Institutes, UCLA School of Medicine, Los Angeles, California 90095-7115; and #INFM UdR Ferrara, Dipartimento di Biologia, Università di Ferrara, 441000 Ferrara, Italy

ABSTRACT We investigated the role of the accessory $\alpha_2\delta$ subunit on the voltage-dependent facilitation of cardiac L-type Ca^{2+} channels (α_{1C}). α_{1C} Channels were coexpressed in *Xenopus* oocytes with β_3 and $\alpha_2\delta$ calcium channel subunits. In $\alpha_{1C} + \beta_3$, the amplitude of the ionic current (measured during pulses to 10 mV) was in average ~1.9-fold larger after the application of a 200-ms prepulse to +80 mV. This phenomenon, commonly referred to as voltage-dependent facilitation, was not observed when $\alpha_2\delta$ was coexpressed with $\alpha_{1C} + \beta_3$. In $\alpha_{1C} + \beta_3$, the prepulse produced a left shift (~40 mV) of the activation curve. Instead, the activation curve for $\alpha_{1C} + \beta_3 + \alpha_2\delta$ was minimally affected by the prepulse and had a voltage dependence very similar to the *G-V* curve of the $\alpha_{1C} + \beta_3$ channel facilitated by the prepulse. Coexpression of $\alpha_2\delta$ with $\alpha_{1C} + \beta_3$ seems to mimic the prepulse effect by shifting the activation curve toward more negative potentials, leaving little room for facilitation. The facilitation of $\alpha_{1C} + \beta_3$ was associated with an increase of the charge movement. In the presence of $\alpha_2\delta$, the charge remained unaffected after the prepulse. Coexpression of $\alpha_2\delta$ seems to set all the channels in a conformational state from where the open state can be easily reached, even without prepulse.

INTRODUCTION

Voltage-dependent calcium channels are heteromultimeric membrane proteins that have been ranked in several classes on the basis of their pharmacological and biophysical properties (see Birnbaumer et al., 1994). The central element of a functional Ca^{2+} channel is the pore-forming α_1 subunit, which is responsible for most of the electrical and pharmacological properties of the channel. The α_1 subunit is physiologically expressed in combination with regulatory subunits (β, $\alpha_2\delta$, and γ), able to modulate several channel functions. As Ca^{2+} fluxes through calcium channels, it controls a number of processes (e.g., cell excitability, muscle contraction, enzyme activity, and gene expression). Therefore, the modulation of the channels by accessory subunits and second messengers becomes a crucial event for cell function. Some of the roles of accessory subunits in channel modulation have been determined using heterologous systems of expression with controlled experimental conditions (e.g., *Xenopus laevis* oocytes) (Neely et al., 1993; Olcese et al., 1994; Felix et al., 1997; Gurnett et al., 1996).

The dihydropyridine (DHP)-sensitive class of calcium channels (L-type) is regulated by neurotransmitters and drugs, and by strong depolarizations. In fact, single strong depolarizations, as well as trains of depolarizations, can induce a transient increase of the channel open probability (facilitation) that persists after the triggering stimulus has ceased. The voltage-dependent facilitation of L-type calcium channels has been described in neurons (Artalejo et al., 1991; Kavalali and Plummer, 1996) in skeletal muscle (Johnson et al., 1994) and in cardiac myocytes (Noble and Shimoni, 1981a, b; Lee, 1987; Fedida et al., 1988; Zygmunt and Maylie, 1990; Pietrobon and Hess, 1990). However, the extent and the kinetic properties of the facilitation greatly vary among different tissues and species, and interestingly, Cens and collaborators (1996) did not find voltage-dependent facilitation in rodent cardiac cells. The expression of cloned calcium channels, with their accessory subunit in simplified expression systems, sheds light on possible reasons for this variability. When the cloned L-type α_{1C} subunit is expressed in *Xenopus* oocytes, its voltage-dependent facilitation appears to be dependent on the type of β subunit coexpressed. Specifically, the facilitation of the L-type channels takes place when the modulatory β_1, β_3, β_4 subunit (Bourinet et al., 1994; Cens et al., 1996, 1998) or the cardiac β_{2a} subunit (Dai et al., 1999) are coexpressed with the pore-forming α_{1C} subunit. On the contrary, in the presence of the palmitoylated form of the β_{2a} subunit (neuronal) facilitation is absent (Cens et al., 1996, 1998; Qin et al., 1998b). In some cases, trains of fast depolarizations resembling action potentials were successfully used to induce facilitation, stressing a physiological role for this phenomenon (Cloues et al., 1997). In this study we show that, besides the involvement of the β subunit, the $\alpha_2\delta$ subunit also modulates the long-lasting voltage-dependent facilita-

Received for publication 4 May 1999 and in final form 7 March 2000.

Address reprint requests to Dr. Riccardo Olcese, Dept. of Anesthesiology, UCLA School of Medicine, BH-509A, CHS, Box 957115, Los Angeles, CA 90095-7115. Tel.: 310-794-7808; Fax: 310-825-6649; E-mail: rolcese@ucla.edu.

Daniela Platano's present address is Dip. Fisiologia Umana e Generale, Universita' di Bologna, 40127 Bologna, Italy.

Ning Qin's present address is Analgesics Research, The R. W. Johnson Pharmaceutical Research Institute, Spring House, PA 19477-0776.

0006-3495/00/06/2959/14 $2.00

tion (Costantin et al., 1998) of a cardiac L-type calcium channel expressed in *Xenopus* oocytes. Although the coexpression of the $\alpha_2\delta$ subunit results in a loss of current potentiation (Dai et al., 1999), the channels seem to behave as if they were constitutively facilitated (Platano et al., 1998). Moreover, we show evidence of an increase in charge movement associated with the facilitation of α_{1C} + β_3, suggesting that a recruitment of silent channels may contribute to the voltage-dependent potentiation. These results have been previously reported in abstract form (Platano et al., 1998).

MATERIALS AND METHODS

RNA synthesis

Throughout our study, the amino terminus deletion mutant (ΔN60) of the rabbit cardiac a_{1C} was expressed in *Xenopus* oocytes. This mutant has a better expression in oocytes than the full-length clone, yielding to larger Ca^{2+} currents without changes in properties (Wei et al., 1996). The α_{1C} pore-forming subunit was expressed in combination with the Ca^{2+} channel accessory subunits β_3 and $\alpha_2\delta$ (Wei et al., 1991; Perez-Reyes et al., 1992). The β_3 and the rabbit skeletal muscle $\alpha_2\delta$ subunits were subcloned into the pAGA2 vector, derived from pGEM-3 (Promega, Madison, WI), containing an alfalfa mosaic virus translational initiation site and a 3′ poly A tail of 92 As to facilitate the expression in *Xenopus* oocytes (Sanford et al., 1991; Wei et al., 1991). Briefly, the full-length cDNA encoding β_3 was amplified by PCR from the original clone in pBS using Pfu DNA polymerase (Stratagene, La Jolla, CA) and primers B2.1 (containing an *Nco*I site) and B2.2 (containing an *Xba*I site). The PCR product was digested with *Nco*I and *Xba*I and subcloned into the pAGA2 vector digested with the same restriction enzymes. The correctness of the constructs was confirmed by DNA sequencing using the dideoxy chain termination method.

To synthesize cRNA, all the constructs were linearized with *Hind*III, followed by treatment with 2 mg/ml proteinase K and 0.5% SDS at 37°C for 30 min to remove traces of activity. After two phenol/chloroform extractions and ethanol precipitation, the templates were suspended in DEPC-treated water to a final concentration of 0.5 μg/μl. cRNAs were in vitro-synthesized at 37°C for 1–2 h in a volume of 25 μl containing 40 mM Tris-HCl (pH 7.2), 6 mM $MgCl_2$, 10 mM dithiothreitol, 0.4 mM each of adenosine triphosphate, guanosine triphosphate, cytosine triphosphate and uridine triphosphate, 0.8 mM 7-methyl guanosine triphosphate, and 10 U T7 RNA polymerase (Boehringer Mannheim, Indianapolis, IN). The transcription products were then extracted with phenol/chloroform, precipitated twice with ethanol, and suspended in DEPC-treated water to a concentration of 0.4 μg/μl. cRNAs for the different subunits (0.2 μg/μl) were mixed in a 1:1 ratio and a volume of 50 nl was injected per oocyte.

Oocyte preparation and RNA injection

Oocytes were obtained from adult female *Xenopus laevis* (from Xenopus One, Ltd., Dexter, MI). Frogs were anesthetized by immersion in water containing 0.15–0.17% tricaine methanesulfonate for ~20 min or until full immobility. The ovaries were removed under sterile conditions by surgical abdominal incision and stage V and VI oocytes were selected. The animals were then killed by decapitation. The animal protocol was performed with the approval of the Institutional Animal Care Committee of the University of California, Los Angeles. One day before injection, oocytes were defolliculated by collagenase treatment (type I, 2 mg/ml for 40 min at room temperature; Sigma, St. Louis, MO). Oocytes were maintained at 19°C in Barth solution supplemented with 50 μg/ml gentamycin. Recordings were done 4–12 days after the RNA injection.

Electrophysiology

The cut-open oocyte voltage clamp technique (Stefani and Bezanilla, 1998) was used to record both ionic and gating currents from oocytes expressing α_{1C} Ca^{2+} channels in combination with the regulatory β_3 and $\alpha_2\delta$ subunits. The composition of the external solution (recording chamber and guard compartments) was 10 mM Ba^{2+}, 96 mM Na^+, and 10 mM HEPES, titrated to pH 7.0 with methanesulfonic acid (MES). The lower chamber in contact with the part of the oocyte permeabilized with 0.1% saponin, contained 110 mM potassium glutamate, and 10 mM HEPES titrated to pH 7.0 with NaOH. Before recording, all the oocytes were injected with 100–150 nl of BAPTA-Na_4 50 mM, titrated to pH 7.0 with MES to prevent activation of endogenous Ca^{2+} and Ba^{2+} activated Cl^- channels (Barish, 1983; Neely et al., 1994). For gating current measurements, the ionic current was blocked by replacing 10 mM Ba^{2+} in the external solution with 2 mM Co^{2+} and 0.2 mM La^{3+}. To remove contaminating nonlinear charge movement related to the oocytes, endogenous Na/K ATPase (Rakovsky, 1993), 0.1 mM ouabain was added to all external solutions. Leakage and linear capacity currents were compensated analogically and subtracted on-line using P/-4 subtraction protocol from −90, −120 mV holding potential (SHP). Charge movement was detected for depolarizations more positive than −70 mV, and no changes were observed using SHPs of either −90 mV or −120 mV. These results indicate that negative subtracting pulses from −90 or −120 mV SHP are adequate to subtract linear components.

Signals were filtered with an eight-pole Bessel filter to one-fifth of the sampling frequency. All the experiments were performed at room temperature (21–23°C).

Data obtained from *Q-V* relationships were fitted with single Boltzmann distribution of the form $Q_{max}/\{1 + \exp[z_1F(V_{(1/2)1} - V_m)/RT]\}$; *G-V* curves were fitted by a dual Boltzmann distribution of the form $G_1/\{1 + \exp[z_1F(V_{half1} - V_m)/RT]\} + G_2/\{1 + \exp[z_2F(V_{half2} - V_m)/RT]\}$, where F and R are the Faraday and gas constant, respectively; T is the absolute temperature; V_{half1} and V_{half2} are the midpoints of activation; z_1 and z_2 are the effective valences; Q_{max} the maximum charge, and G_1 and G_2 are the amplitudes of the first and the second components of the distribution. All data are reported as mean values ± SEM.

RESULTS

Effect of the $\alpha_2\delta$ modulatory subunit on α_{1C} β_3

Cardiac α_{1C} calcium channels and the auxiliary calcium channel β_3 subunit were expressed in *Xenopus* oocytes with and without the $\alpha_2\delta$ subunit. The expression of α_{1C} + β_3 and α_{1C} + β_3 + $\alpha_2\delta$ gave rise to large ionic currents having different properties, depending on the channel subunit composition. Representative traces obtained from the combinations α_{1C} + β_3 (*A*) and α_{1C} + β_3 + $\alpha_2\delta$ (*B*) are shown in Fig. 1. The currents were elicited by depolarization to −30 mV, 0 mV, and +30 mV from −90 mV holding potential (HP). As previously described by other authors (Bangalore et al., 1996; Felix et al., 1997; Qin et al., 1998a) the coexpression of the $\alpha_2\delta$ subunit increased the peak current, shifted the current-voltage (*I-V*) curve peak 10 mV to more negative potential, and increased the activation and deactivation rates of α_{1C} + β_3. These modulatory effects were used as a positive control for the good expression of the $\alpha_2\delta$ subunit. When the *I-V* curves of α_{1C} + β_3 and α_{1C} + β_3 + $\alpha_2\delta$ are normalized to the peak inward current (Fig. 1 *C*), the magnitudes of the outward currents are markedly dif-

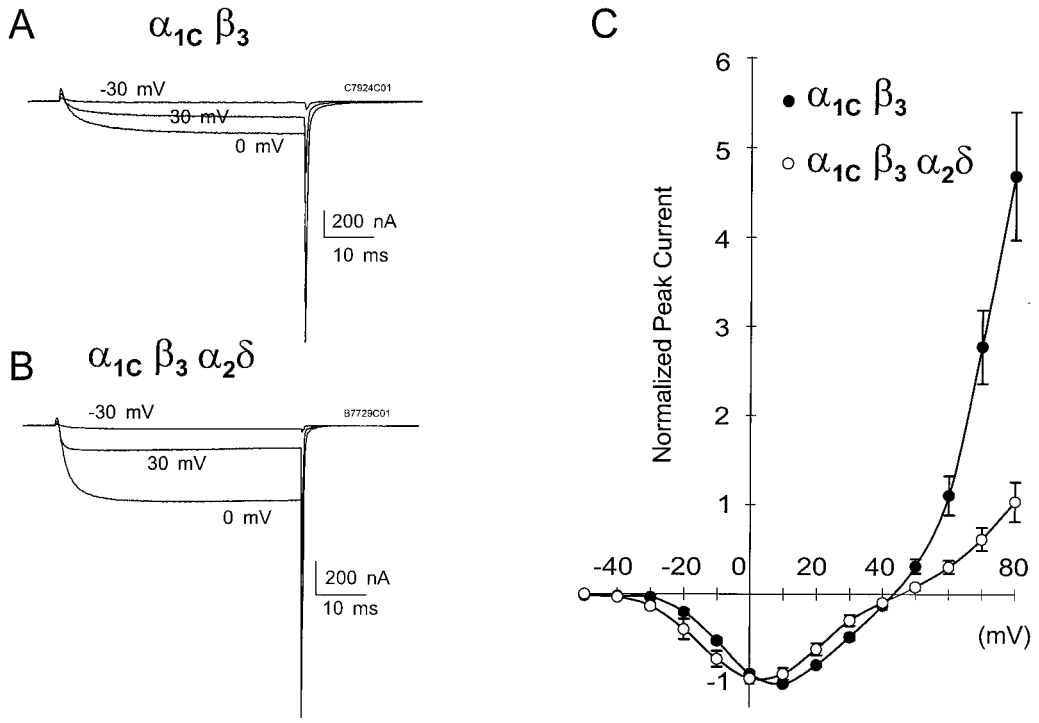

FIGURE 1 Comparison of voltage-dependent properties of α_{1C} when expressed in combination with β_3 and $\beta_3 + \alpha_2\delta$. Representative current families from either $\alpha_{1C} + \beta_3$ (*A*) and $\alpha_{1C} + \beta_3 + \alpha_2\delta$ (*B*) elicited stepping from −50 mV to +50 mV in 10-mV increments. The holding potential was −90 mV. In (*C*) are shown normalized *I-V* curves for $\alpha_{1C} + \beta_3$ (●, $n = 9$) and $\alpha_{1C} + \beta_3 + \alpha_2\delta$ (○, $n = 6$).

ferent, while the reversal potentials are practically identical. In the presence of the $\alpha_2\delta$ subunit, the outward current had a shallower voltage dependence relative to $\alpha_{1C} + \beta_3$.

Effect of a strong depolarization on the ionic currents carried by $\alpha_{1C} + \beta_3$ and $\alpha_{1C} + \beta_3 + \alpha_2\delta$

We studied the facilitation of the ionic current of α_{1C} using a double-pulse protocol. The current was recorded during a pulse to 10 mV before and after the application of a 200-ms prepulse to +80 mV (the protocol is shown on the top panel of Fig. 2). Although the α_{1C} current did not show potentiation after the prepulse, currents recorded from oocytes expressing $\alpha_{1C} + \beta_3$ were facilitated when preceded by a positive prepulse (200 ms at +80 mV; Fig. 2, *A* and *B*). The potentiation observed for this subunit composition lasted several seconds after the prepulse during a repolarization to −90 mV. In Fig. 2, panels *A* and *B* show the current facilitation of the subunit composition $\alpha_{1C} + \beta_3$ after a 200-ms prepulse to 80 mV followed by repolarization of 50 ms (*A*) and 1 s (*B*) to −90 mV. To estimate the duration of the facilitation, the averaged peak facilitated currents (recorded during the test pulse at 10 mV) were plotted versus time of repolarization to −90 mV (interpulse). The facilitation decayed following a double-exponential time course with time constants of 0.44 s and 51.38 s. The amplitudes of the two components were, respectively, 55% and 45% of the total facilitation ($n = 8$, Fig. 2 *E*).

When $\alpha_{1C} + \beta_3$ was expressed together with the $\alpha_2\delta$ subunit, the current potentiation induced by the prepulse was no longer observed, as shown by the representative current traces in Fig. 2, *C* and *D*. In this case, the turn-on of the ionic currents was faster and showed a time-dependent decay. For very brief repolarizations (<50 ms) the current during the test pulse was slightly reduced after the positive prepulse, possibly due to inactivation. Fig. 2 *F* shows the lack of potentiation in $\alpha_{1C} + \beta_3 + \alpha_2\delta$: the potentiation after a 200-ms prepulse to 80 mV is plotted against the time of repolarization at −90 mV (*D*, $n = 11$). Even stronger prepulses (up to 140 mV) did not elicit potentiation in the presence of the $\alpha_2\delta$ subunits (data not shown).

Effect of prepulses on the voltage dependence of the activation in $\alpha_{1C} + \beta_3$ and $\alpha_{1C} + \beta_3 + \alpha_2\delta$

By comparing the voltage dependence of the activation (*G-V* curve) in $\alpha_{1C} + \beta_3$ and $\alpha_{1C} + \beta_3 + \alpha_2\delta$, and the modulatory effect of positive prepulses, we examined the possibility that the addition of the $\alpha_2\delta$ subunit already maximized channel opening, leaving no room for the potentiation process to occur. In this study we used 25-ms depolarizing steps, ranging from −80 to 190 mV in 10-mV

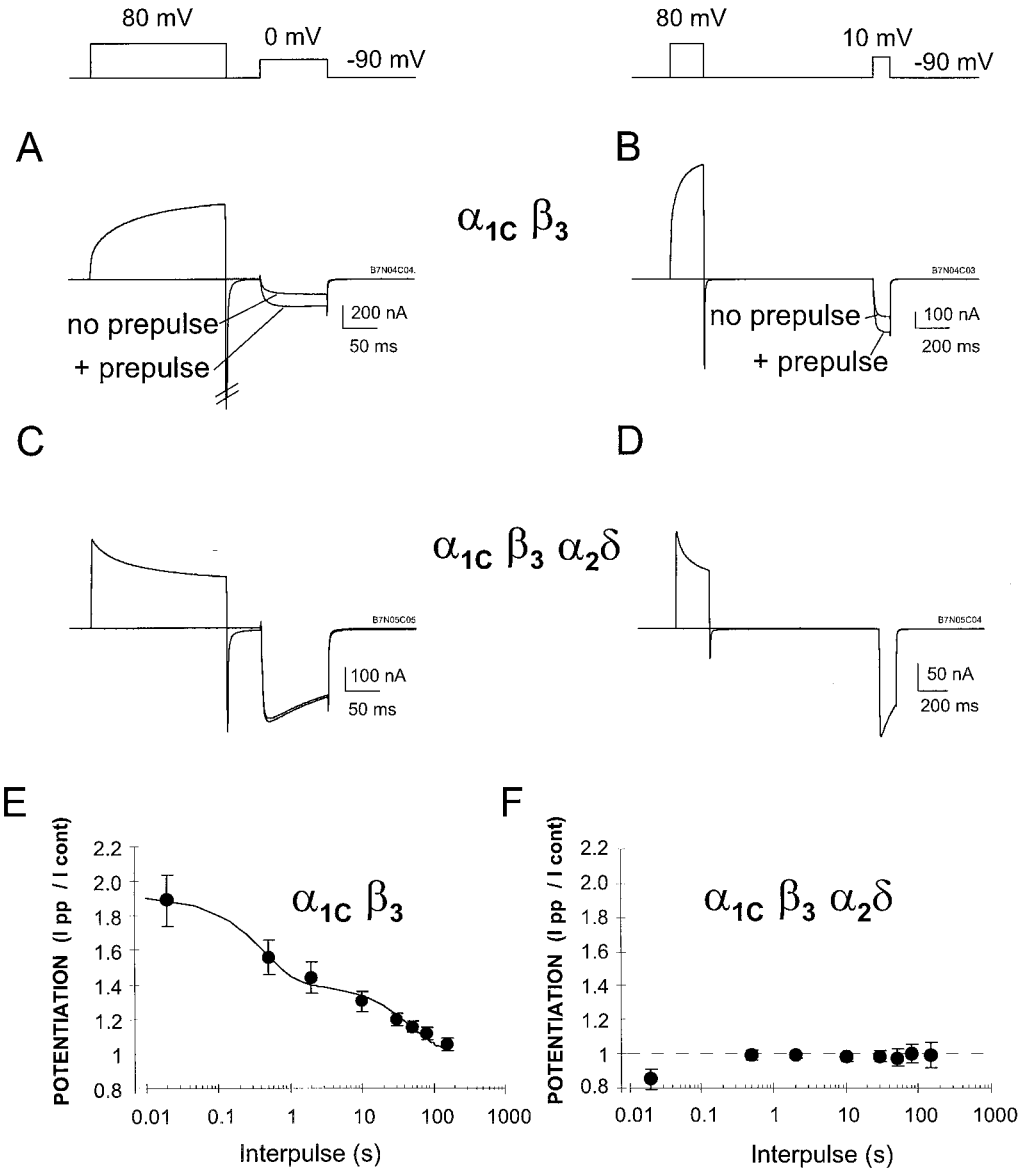

FIGURE 2 The $\alpha_2\delta$ subunit seems to prevent prepulse potentiation. (*A*) $\alpha_{1C} + \beta_3$ superimposed current traces evoked by the voltage protocol shown at top. The current during a 10-mV test pulse increases when the test pulse is preceded by a prepulse to 80 mV. The potentiation is long-lasting and still present after a 1-s repolarization to −90 mV (*B*); the voltage protocols are shown above the current traces. When $\alpha_{1C} + \beta_3$ is expressed together with $\alpha_2\delta$, there is no significant potentiation of the current (*C*) and (*D*). (*E*) The extent of potentiation of the ionic current at 10 mV is plotted versus the time of repolarization between the prepulse and test pulse for the combination $\alpha_{1C} + \beta_3$. The potentiation decayed in a double-exponential manner with time constants of $\tau_{fast} = 0.44$ s, $Amp_{fast} = 50.1\%$, and $\tau_{slow} = 51.38$, $Amp_{slow} = 40.8\%$ s, $n = 8$. No significant potentiation was measured by coexpressing the $\alpha_2\delta$ subunit (*F*) ($n = 6$).

increments, followed by a repolarization to −50 mV delivered every 5 s. The *G-V* curves were constructed plotting the peak tail currents at −50 mV against the potentials of the depolarizing steps. The voltage steps were delivered in control conditions (i.e., without prepulse) (Fig. 3 *A*) or preceded by a 200-ms prepulse to 80 mV (Fig. 3 *B*). The recovery from potentiation was measured without prepulses 2–3 min later (Fig. 3 *C*). As described in Fig. 2, the prepulse increased the ionic current during the test pulse in $\alpha_{1C} + \beta_3$: Fig. 3 *D* shows the *I-V* plot for control (●) and potentiated current (○) obtained by measuring the values of the ionic current at the end of the 25-ms test pulse.

The normalized averaged *G-V* curves ($n = 9 \pm$ SEM) show that the overall effect of the prepulse is to shift the voltage dependence of channel activation to more negative potentials (Fig. 3 *E*). The data could be fitted in both control (●) and potentiated (○) *G-V* values with the sum of two Boltzmann distributions with the same half-activation po-

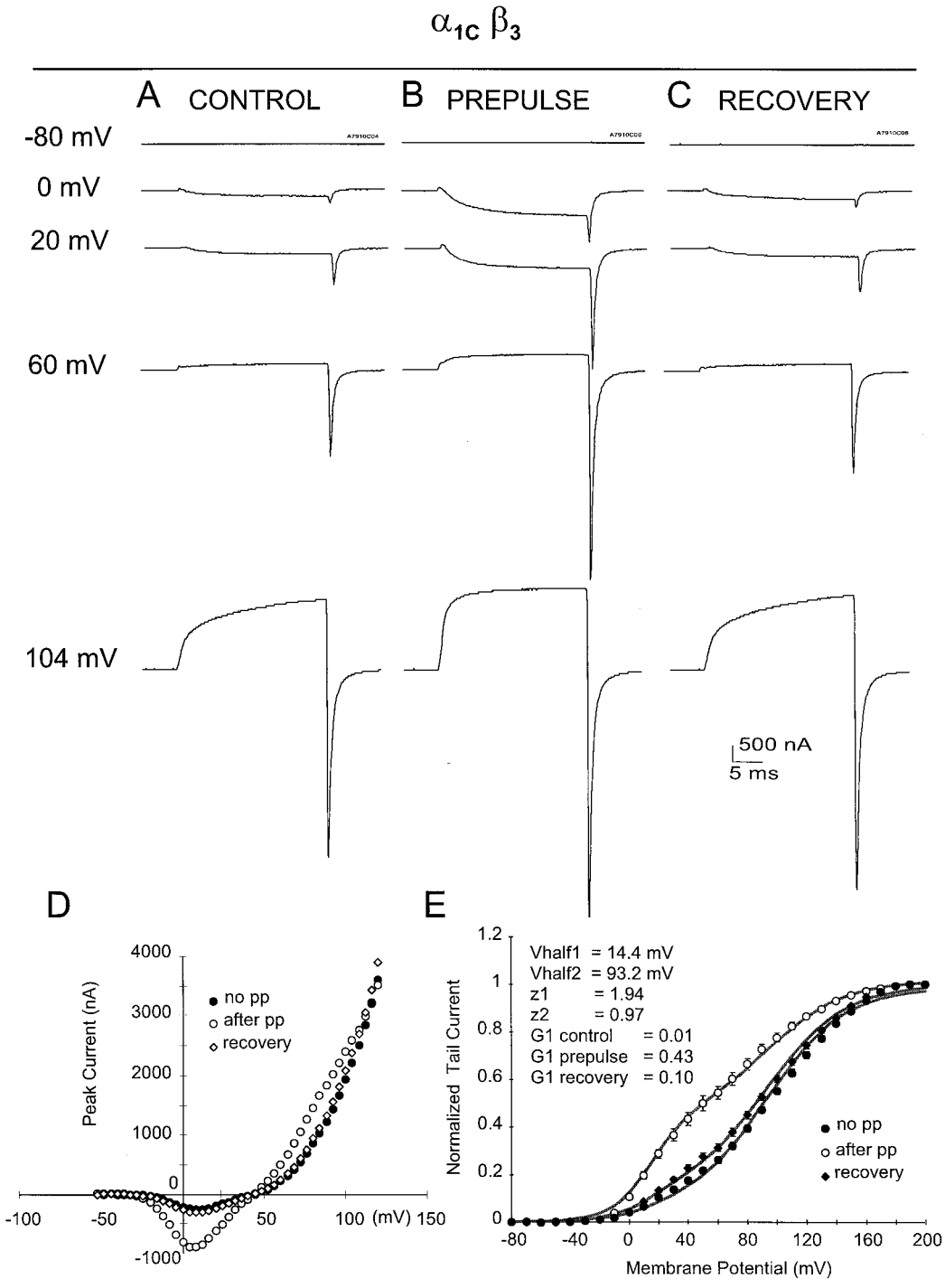

FIGURE 3 In $\alpha_{1C} + \beta_3$, a positive prepulse shifts the activation curve to more negative potentials. Three families of Ba^{2+} currents were recorded from an oocyte expressing $\alpha_{1C} + \beta_3$. Representative traces are shown for a 25-ms depolarization to the indicated potentials; tails currents are evoked by repolarization to −50 mV. (*A*) Ionic currents recorded in the absence of a preceding prepulse. (*B*) the depolarizing steps were preceded by a 200-ms prepulse to 80 mV, followed by a repolarization (interpulse) of 50 ms to −90 mV. Both ionic and gating currents increased in amplitude. (*C*) The same conditions as in (*A*); the test protocol without prepulse was run 2 min after the experiment shown in (*B*). (*D*) Current-voltage relationships from the same oocyte. Note that the *I-V* curve recorded in the absence of prepulse merged with the potentiated one for potentials above 100 mV. (*E*) Averaged normalized *G-V* curves measured from the tail currents during the repolarization to −50 mV ($n = 9$) for Ba^{2+} current recorded in control (●), after a 200-ms prepulse to +80 mV (○), and during the recovery (◆). Error bars represent SEM. Data were fitted by dual Boltzmann distributions (see Methods).

tentials and slope factors, and with different proportion of the relative amplitudes of the two components. The positive prepulse increased the fraction of the more negative components from 1% to 43% of the total conductance, resulting in an overall negative shift of the *G-V* curve. The *G-V* curves are shown normalized to their maxima. The operation was required because of the progressive time-dependent rundown of the conductance, which was enhanced by the demanding pulse protocol. However, as assessed by the experiments shown in Fig. 4, in which the channels were challenged by only two test voltages (to prevent the rundown), the limiting conductance of $\alpha_{1C} + \beta_3$ (measured with a pulse to 180 mV) was the same with or without prepulse.

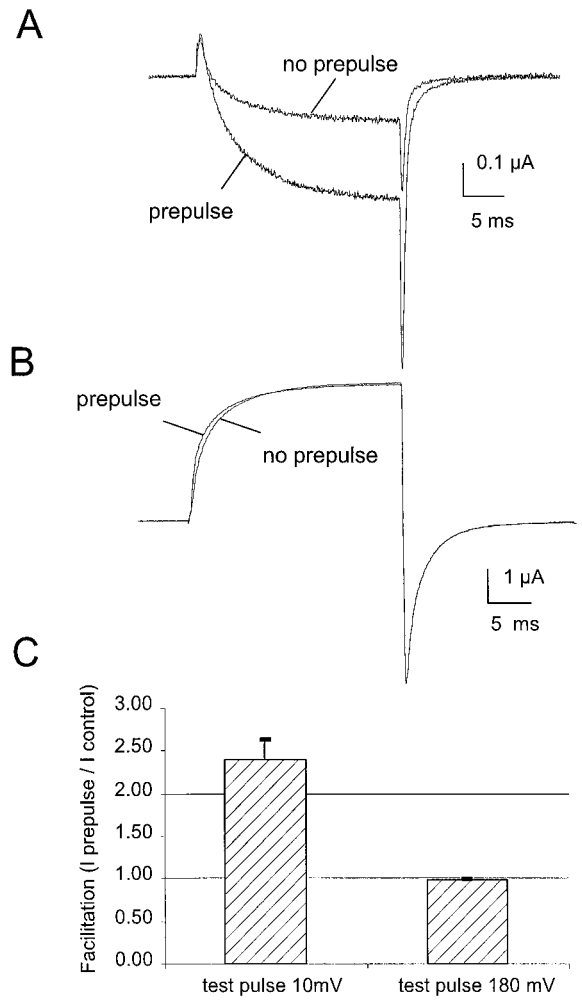

FIGURE 4 The limiting conductance of $\alpha_{1C} + \beta_3$ does not change with the prepulse. Current records from an oocyte expressing $\alpha_{1C} + \beta_3$, evoked by two test pulses to +10 mV (*A*) and +180 mV (*B*), preceded or not by a prepulse of 200 ms to +80 mV. Note the lack of further potentiation when the test pulse is +180 mV (*B*). The bar plot in (*C*) summarizes the degree of facilitation induced by the prepulse as measured during a test pulse to +10 and +180 mV ($n = 6$). The oocytes were challenged with a minimum number of pulses to minimize the rundown of the current. The conditions and the pulse protocol are the same as in Fig. 3.

In oocytes expressing $\alpha_{1C} + \beta_3 + \alpha_2\delta$, no potentiation of the ionic currents was detected after the positive prepulse (Fig. 5, *A–C*). The *I-V* curves of a representative oocyte are shown in Fig. 5 *D* (■, Control; □, Prepulse). The normalized *G-V* curves obtained from oocytes expressing $\alpha_{1C} + \beta_3 + \alpha_2\delta$ revealed a little effect of the prepulse on the voltage dependency of the channel activation. The *G-V* curve in $\alpha_{1C} + \beta_3 + \alpha_2\delta$ without prepulse (■) was practically identical to the *G-V* curve obtained for the combination $\alpha_{1C} + \beta_3$ after the positive prepulse (Fig. 5 *E*, *dashed line*). The dotted line corresponds to the fit of *G-V* curve of $\alpha_{1C} + \beta_3$ without prepulses. We simultaneously fitted all *G-V* curves for both $\alpha_{1C} + \beta_3$ and $\alpha_{1C} + \beta_3 + \alpha_2\delta$, with and without the prepulse, to the same effective valences (z_1 and z_2) and half-activation potentials (V_{half1} and V_{half2}) for the two components, but with a different proportion of their amplitude factors. The effective valences z_1 and z_2 were 1.94 for the first, more negative component, and 0.97 for the second, more positive component. The half-activation potentials (V_{half1} and V_{half2}) were 14.4 mV and 93.2 mV, respectively. As mentioned for $\alpha_{1C} + \beta_3$ injected oocytes, the first component of the *G-V* (G_1) increased after the prepulse from 1% of the G_{max} (in control) to 43% (Fig. 3 *E*). However, when $\alpha_2\delta$ was coexpressed with $\alpha_{1C} + \beta_3$, the proportion of G_1 was already 53% in control conditions and the prepulse had a minor effect on the ratio between the two amplitudes of the fit ($G_1 = 67\%$ with prepulse). These findings suggest that the presence of the $\alpha_2\delta$ sets the channels in a conformational state similar to the one reached after prepulse potentiation.

Facilitation develops during positive pulses in $\alpha_{1C} + \beta_3$

The installation of outward ionic current is much faster in $\alpha_{1C} + \beta_3 + \alpha_2\delta$ than in $\alpha_{1C} + \beta_3$. The slow component of the outward current $\alpha_{1C} + \beta_3$ probably reflects the development of the potentiation occurring during the pulse. We used a 200-ms test pulse to 80 mV preceded by an identical prepulse to test this possibility. As shown in Fig. 6 *A*, the outward current in $\alpha_{1C} + \beta_3$ during a control pulse to 80 mV develops with a relatively slow kinetic. When a prepulse to 80 mV is applied, the current during the same test pulse to 80 mV develops with a much faster kinetic. The two current traces (with and without prepulse) merge together at the end test pulse, indicating that a ~150-ms pulse is sufficient to induce the maximal potentiation at 80 mV. On the contrary, the coexpression of the $\alpha_2\delta$ produces a fast developing ionic current which is virtually unmodified by positive prepulse (Fig. 6 *B*).

Effect of prepulse on gating current amplitude recorded at the ionic current reversal potential

Voltage-dependent calcium channels respond to changes in the potential across the plasma membrane by changing their

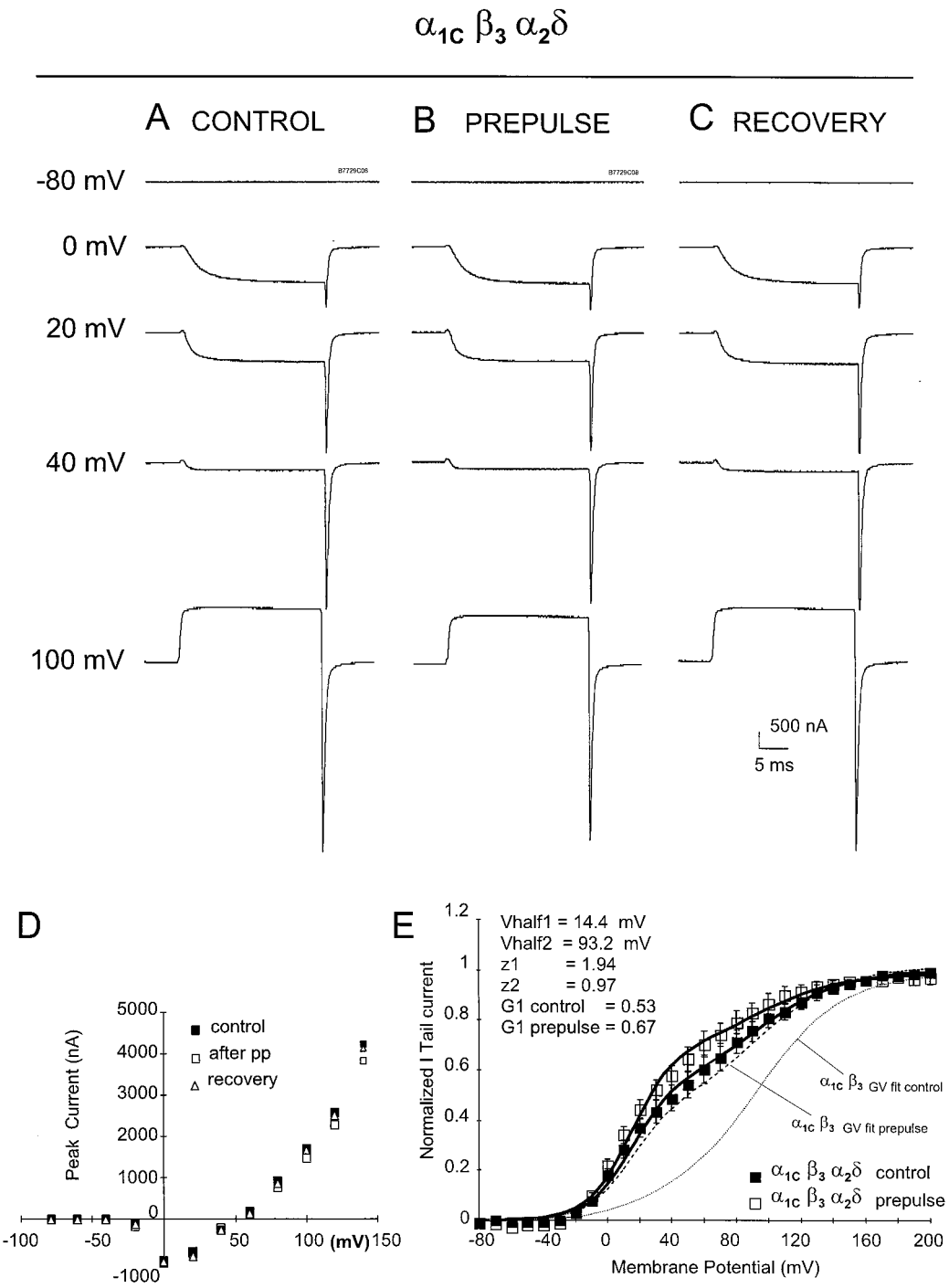

FIGURE 5 In $\alpha_{1C} + \beta_3 + \alpha_2\delta$, a positive prepulse has little effect on the activation curve. Current records from an oocyte expressing $\alpha_{1C} + \beta_3 + \alpha_2\delta$ are shown. Twenty-five-millisecond depolarizations to the indicated potentials were delivered in control condition (without prepulse) (*A*) after a 200-ms prepulse to +80 mV (*B*) and 2 min after the prepulse protocol (*C*). The time of repolarization between the prepulse and the test pulse was 50 ms at −90 mV. In (*D*) is shown the *I-V* relationship for the same oocyte in control (■), after the prepulse (□), and after the recovery (△). (*E*) Averaged and normalized GV curves measured from the tail currents during the repolarization to −50 mV ($n = 6$) for Ba^{2+} current recorded in control (■) and after a 200-ms prepulse to +80 mV (□). The solid lines are the simultaneous fit to the sum of two Boltzmann distributions. In the plot are also reported the *G-V* fits of $\alpha_{1C} + \beta_3$ without the prepulse (*dotted line*) and after prepulse (*dashed line*) as shown in Fig. 3. Error bars are SEM.

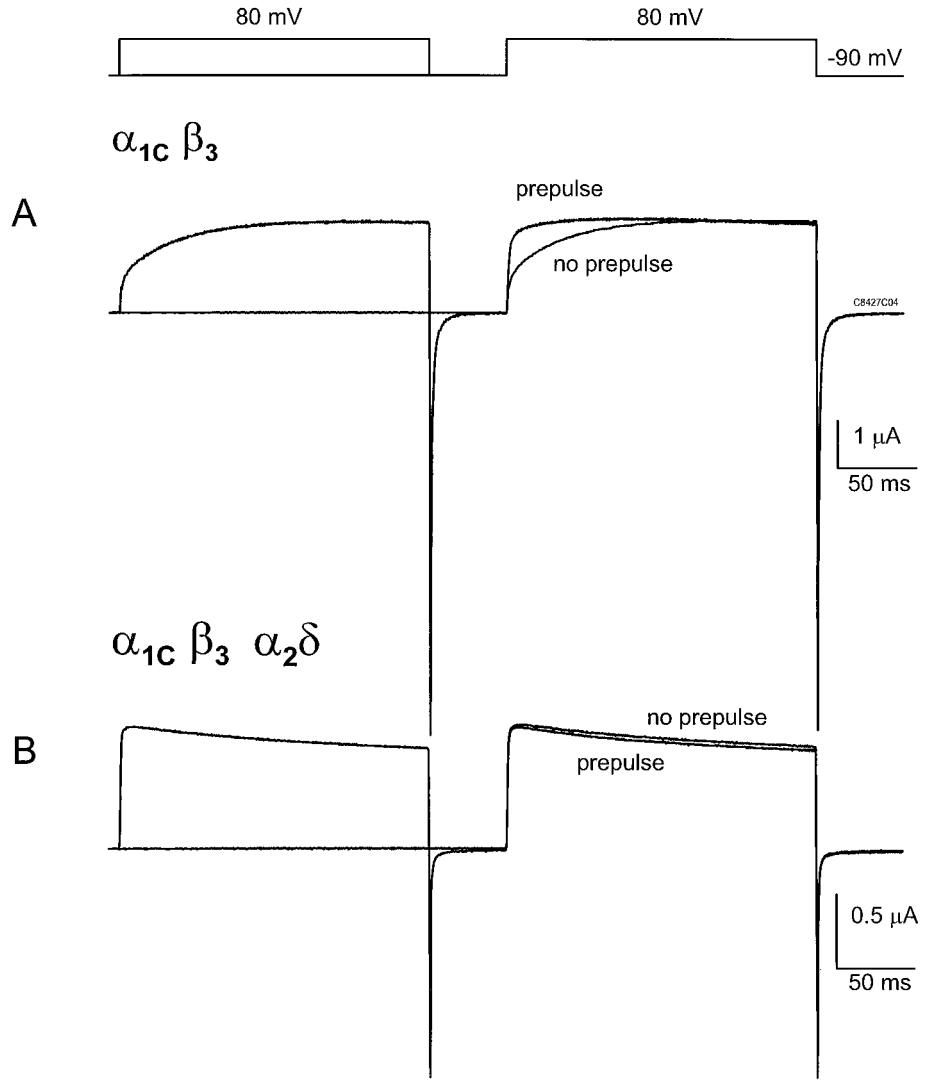

FIGURE 6 Differential effect of a 200-ms prepulse to +80 mV on the ionic current from $\alpha_{1C} + \beta_3$ and $\alpha_{1C} + \beta_3 + \alpha_2\delta$. (*A*) Two superimposed current traces elicited by a double pulse voltage protocol shown in the top panel. In $\alpha_{1C} + \beta_3$, the current elicited by a test pulse to 80 mV develops slowly. The activation kinetics of a pulse to 80 mV is greatly accelerated by the application of a 200-ms prepulse to the same potential. After the positive prepulse, the current in the test pulse is already potentiated, as shown by the faster kinetics. Instead, the coexpression with $\alpha_2\delta$ (*B*) elicited a fast-rising current during the test pulse at 80 mV (without prepulse), and remains practically unmodified after the prepulse.

conformational state and giving rise to the gating currents. Thus, the amplitude of gating current is proportional to the number of channels able to gate. To have a simultaneous evaluation of the behavior of the gating current and the change in membrane conductance induced by the prepulse, we recorded the currents at the reversal potential using the standard external solution containing 10 mM Ba^{2+} (Fig. 7). By pulsing at the reversal potential, it is possible to record the "ON" gating currents at the beginning of the depolarizing pulse and the ionic tail current partially contaminated by the "OFF" gating current at the end of the pulse, during the repolarization. The experimental reversal potential, ranging from +45 mV to +55 mV, was determined for each experiment. We found that after the delivery of a 200-ms prepulse to 60 mV in the oocytes expressing $\alpha_{1C} + \beta_3$, the facilitation of the ionic current (as assessed by the increase in the tail current) was accompanied by an increase of the ON charge measured at the reversal potential. Fig. 7 *A* shows superimposed ON gating and tail currents of $\alpha_{1C} + \beta_3$, recorded without prepulses and after 50-ms repolarization to −90 mV following a 200-ms prepulse to 60 mV. Both gating and tail currents increased in magnitude after the prepulse. Some degree of facilitation of gating and ionic currents remained when the repolarization time was increased to 1 s (Fig. 7 *B*). The insets in Fig. 7, *A* and *B* show enlarged gating currents. The solid lines represent time integrals of the gating currents recorded in the absence of prepulse, while dashed lines are the time integrals of the gating currents recorded after the 200-ms prepulse to 60 mV. Clearly, the prepulse was able to enhance the total charge moved at the beginning of the depolarization.

After the coexpression of the $\alpha_2\delta$ subunit ($\alpha_{1C} + \beta_3 + \alpha_2\delta$), an equivalent pulse protocol failed to produce an increase of both gating and ionic currents (Fig. 7, *C* and *D*). Instead, both the gating and ionic current (tail) amplitudes were slightly reduced when the repolarizing interpulse was

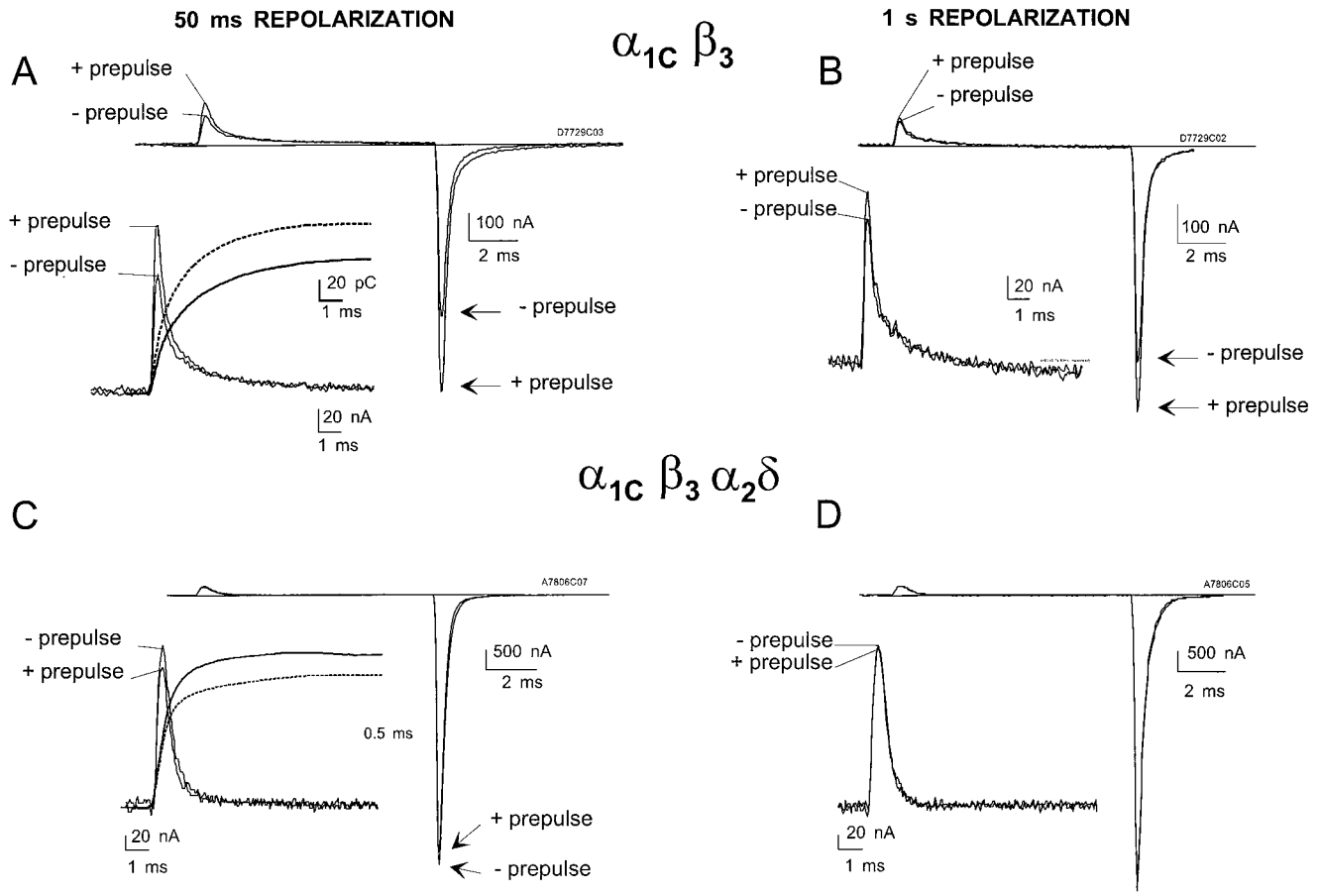

FIGURE 7 Increase in charge movement and tail current after prepulse in $\alpha_{1C} + \beta_3$, and effect of the $\alpha_2\delta$ subunit. In oocytes expressing $\alpha_{1C} + \beta_3$ and $\alpha_{1C} + \beta_3 + \alpha_2\delta$, gating and ionic tail currents were simultaneously recorded pulsing to the reversal potential. The external solution contained 10 mM Ba^{2+}. (*A*) and (*B*) show superimposed current traces recorded from the same oocyte expressing $\alpha_{1C} + \beta_3$ before and after a 200-ms prepulse to 60 mV. In (*A*) the time of repolarization between the prepulse and the test pulse was 50 ms, while in (*B*) it was 1 s. The ON gating currents are magnified and their time integrals are shown. Solid lines represent time integrals of the gating currents recorded in the absence of prepulse; dashed lines are the time integrals of the gating currents recorded after the prepulse. The arrows indicate the amplitude of the tail currents recorded in the absence (−prepulse) or after (+prepulse) the prepulse. Notice that an increase in charge movement after the prepulse is accompanied by an increase in the tail current. (*C*) and (*D*) are current traces recorded from the same oocyte expressing $\alpha_{1C} + \beta_3 + \alpha_2\delta$ before and after a 200-ms prepulse to 60 mV. The repolarization time between the prepulse and the test pulse was 50 ms (*C*) and 1 s (*D*). A small decrease in charge movement and a corresponding decrease in tail current occurred when the $\alpha_2\delta$ subunit was coexpressed.

50 ms long (Fig. 7 *C*). The reduction in charge movement was probably due to the occupancy of closed states nearer to the open state on the activation pathway, because the short repolarizing interpulse was not long enough to allow for the re-population of the deepest closed states. For longer repolarization times, the gating and ionic currents were identical with and without prepulses (Fig. 7 *D*).

The time course of the decaying phase of the gating current was not significantly modified by the prepulse. The gating current decays were fitted with a double-exponential function. In $\alpha_{1C} + \beta_3$, τ_{fast} and τ_{slow} were, respectively, 0.42 ± 0.04 ms and 3.98 ± 0.99 ms without prepulse, and 0.41 ± 0.06 ms and 3.44 ± 0.88 ms after the prepulse. In $\alpha_{1C} + \beta_3 + \alpha_2\delta$, τ_{fast} and τ_{slow} were, respectively, 0.44 ± 0.06 ms and 5.39 ± 1.84 ms without prepulse, and 0.39 ± 0.05 ms, 5.39 ± 1.84 after the prepulse. The fast component of the total charge was predominant (87% for $\alpha_{1C} + \beta_3$ and 92% for $\alpha_{1C} + \beta_3 + \alpha_2\delta$).

The prepulse does not change the voltage dependence of gating currents

In order to better characterize the effect of prepulses on gating currents, we blocked the ionic conductance by replacing Ba^{2+} in the external solution with 2 mM Co^{2+} and 0.2 mM La^{3+}. Similar to the experiments for the facilitation of the ionic current, we used 200-ms prepulses to 80 mV. In $\alpha_{1C} + \beta_3$-expressing oocytes, the prepulse produced an increase of charge movement at all of the tested potentials.

Fig. 8 shows gating current traces (*solid lines*) and their time integral (*dashed lines*) from an oocyte expressing $\alpha_{1C} + \beta_3$, recorded by stepping to the indicated potential from −90 mV holding potential in control condition (without prepulse, Fig. 8 *A*) and after a 200-ms prepulse to 80 mV (Fig. 8 *B*). Both ON and OFF gating currents were larger after the prepulses (*B*). The increase in charge movement was transient and recovered after holding the oocytes at −90 mV for ~2 min (Fig. 8 *C*). We constructed *Q-V* curves by integrating the ON gating current measured during depolarizations between −80 and +70. Above 70 mV the isolation of the gating current could not be adequately maintained due to the contaminating outward ionic current. In oocytes expressing $\alpha_{1C} + \beta_3$, the charge increased ~20% after the prepulse (Fig. 8 *D*). The *Q-V* curves for control, prepulse, and recovery were simultaneously fitted by a single Boltzmann distribution (*solid lines*) with a half-activation potential (V_{half}) = −9.9 mV and effective valence (z) = 1.4. The normalized maximum charge displacement after the prepulse increased by ~20% compared to the control. No significant changes in the kinetic properties and voltage dependence of gating current were detected after the prepulses (Fig. 8 *E*).

Similarly to the ionic current, the gating current of oocytes expressing $\alpha_{1C} + \beta_3 + \alpha_2\delta$ did not increase with the prepulse (Fig. 9, *A* and *B*). Instead, gating current amplitudes recorded after the 200-ms prepulse to 80 mV (Fig. 9 *B*) were slightly reduced in respect to the gating current recorded in the absence of prepulse (Fig. 9 *A*). The *Q-V* curves obtained by integrating the ON gating current showed a small reduction of the maximum charge displacement when the positive prepulse was applied (Fig. 9 *D*). This small reduction was fully recovered in <1 s at −90 mV.

As for $\alpha_{1C} + \beta_3$, the normalized *Q-V* curves from $\alpha_{1C} + \beta_3 + \alpha_2\delta$ were simultaneously fitted by a single Boltzmann function having V_{half} = −2.29 mV, z = 1.81, with a reduction of ~7% in Q_{max} in the presence of the prepulse (Fig. 9 *D*). No significant changes in the voltage dependence were observed after the prepulse (Fig. 9 *E*).

DISCUSSION

Prepulse facilitation and phosphorylation

The voltage-dependent facilitation of the L-type Ca^{2+} current has been observed in a variety of tissues and cell lines. Although several studies concluded that cAMP-dependent phosphorylation is not involved in the voltage-dependent facilitation of L-type current, in some cases it has been shown the opposite (for a review see Dolphin, 1996). Some authors reported that the enhancement of the current level via the activation of PKA was not observed in the *Xenopus* oocyte expression system, probably because of the high basal level of PKA activity in oocytes (Singer-Lahat et al., 1994).

The voltage-dependent facilitation described in the present work was not significantly affected by altering the kinase activity of the oocytes. Injection of the non-hydrolyzable cAMP analog Rp-cAMP (100 nl, 0.2 mM or 2 mM, n = 10), with and without BAPTA, 0.5 to 3 h before voltage clamp recording, did not cause significant changes in the prepulse facilitation (data not shown). Similarly, the cAMP-dependent PK inhibitor (6–22 amide) injected 10 min before recording (100 nl, 20 μM) did not prevent long-lasting facilitation (n = 3, data not shown). This result supports the hypothesis that the long-lasting facilitation of $\alpha_{1C} + \beta_3$ is due to a structural change induced by strong depolarizations that set the channel in a conformational state more responsive to voltage. In agreement with the recent work of Dai and collaborators (1999), prepulse facilitation does not seem to require cAMP-dependent phosphorylation.

Some aspects of prepulse facilitation in L-type calcium channels resemble the characteristic voltage-dependent block by the G-protein of N- and E-type Ca^{2+} channels. The binding of the G-protein $\beta\gamma$ subunit to the Ca^{2+} channel is voltage-dependent. Strong depolarizations relieve the block, leading to an increase in open probability of the channels (Bean, 1989; Ikeda, 1996) resulting in facilitation. Although cardiac α_{1C} channels expressed in oocytes are not modulated by G-protein (Qin et al., 1997), it is possible that a mechanism similar to the one mentioned is responsible for the long-lasting voltage-dependent facilitation of $\alpha_{1C} + \beta_3$. The tonic inhibition of an unidentified molecule would be relieved by the strong depolarizations, yielding to the facilitation: the extremely slow ON rate of the rebinding of the blocking particle could be the reason for the long-lasting characteristic of the facilitation.

$\alpha_2\delta$ Seems to mimic prepulse facilitation

The coexpression of the $\alpha_2\delta$ subunit seems to prevent the voltage-dependent facilitation of $\alpha_{1C} + \beta_3$. The analysis of the voltage dependence of the activation suggests that the channels expressed with the $\alpha_2\delta$ subunits behave as if they were constitutively potentiated. In fact, the *G-V* curve of $\alpha_{1C} + \beta_3 + \alpha_2\delta$ is shifted to the left and its voltage dependence strictly follows the voltage dependence of the $\alpha_{1C} + \beta_3$ channels when they are potentiated by the prepulse. The positive prepulse has only a very small effect on the *G-V* curves of channels expressed with $\alpha_2\delta$. An appealing interpretation of this result is the lack of room for channel potentiation, because the activation curve is already fully shifted to the left on the voltage axis. However, it should also be taken into consideration that in $\alpha_{1C} + \beta_3$, the limiting G_{max} with and without prepulse tends to maintain the same value. This could be due either to the fact that the limiting open probability cannot be further increased by the prepulse, or because of a rapidly developing facilitation at

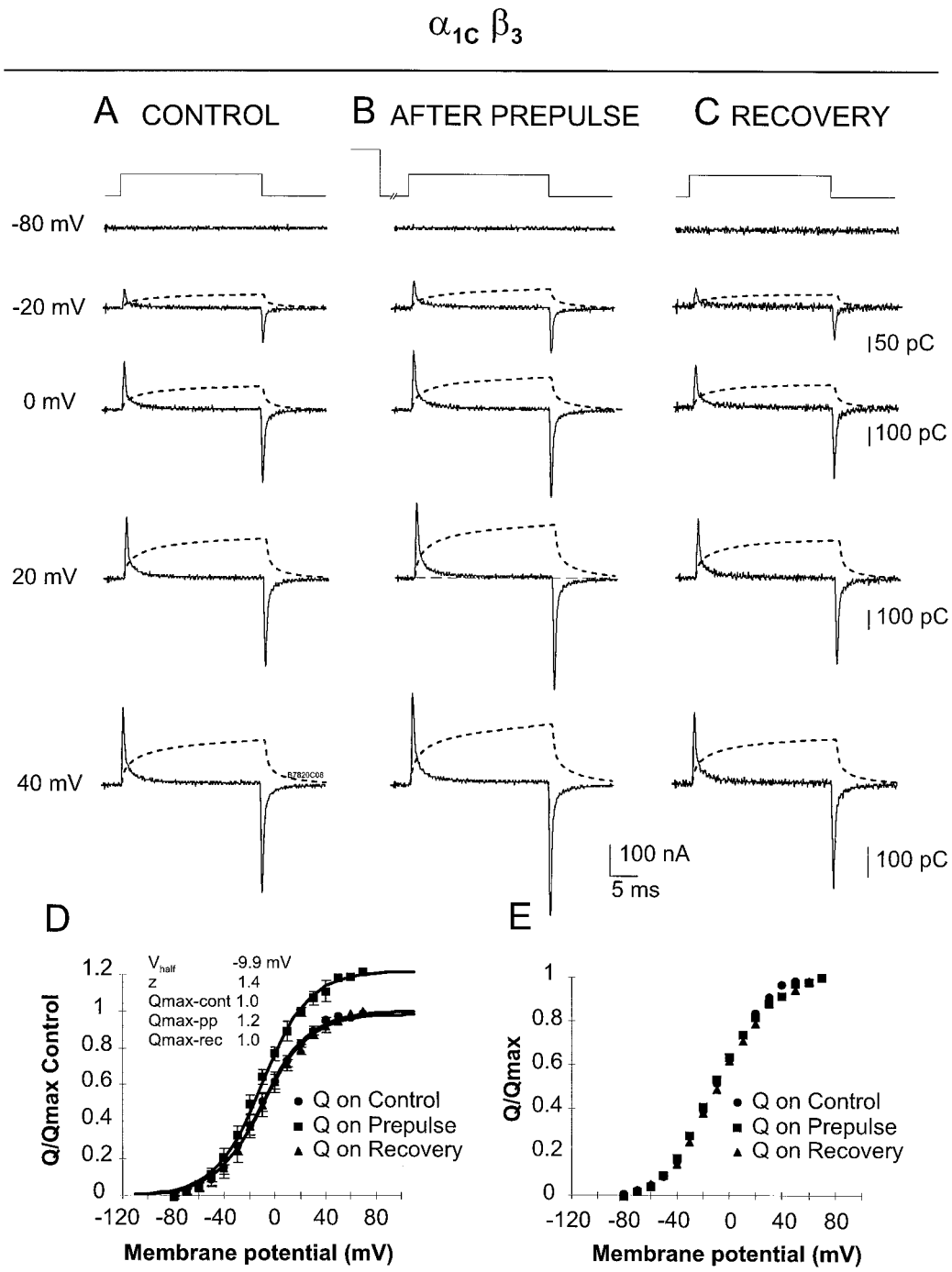

FIGURE 8 Prepulse effect on gating current in $\alpha_{1C} + \beta_3$. $\alpha_{1C} + \beta_3$ Gating current traces during 30-ms depolarization to the indicated potentials are shown. The ionic current was blocked by external 2 mM Co^{2+} and 0.2 mM La^{3+}. (*A*) Gating currents recorded in the absence of a positive prepulse. In (*B*) the depolarizing steps were preceded by a 200-ms prepulse to +80 mV followed by a 50-ms repolarization to −90 mV. (*C*) Same conditions as in (*A*); the protocol for the recovery was applied 2 min after the prepulse experiment. Dashed lines represent the time integrals of the gating currents. (*D*) Averaged *Q-V* curves (Q_{ON}) obtained from gating currents recorded in control conditions (■), after a 200-ms prepulse to +80 mV (●), and during the recovery (▲) ($n = 5$ oocytes). Error bars represent SEM. Solid lines are the simultaneous fits to a single Boltzmann distribution. Parameters used for the fitting are shown in the plot. (*E*) Normalized *Q-V* curves (same as in *D*): control (●), prepulse (■), and recovery (▲).

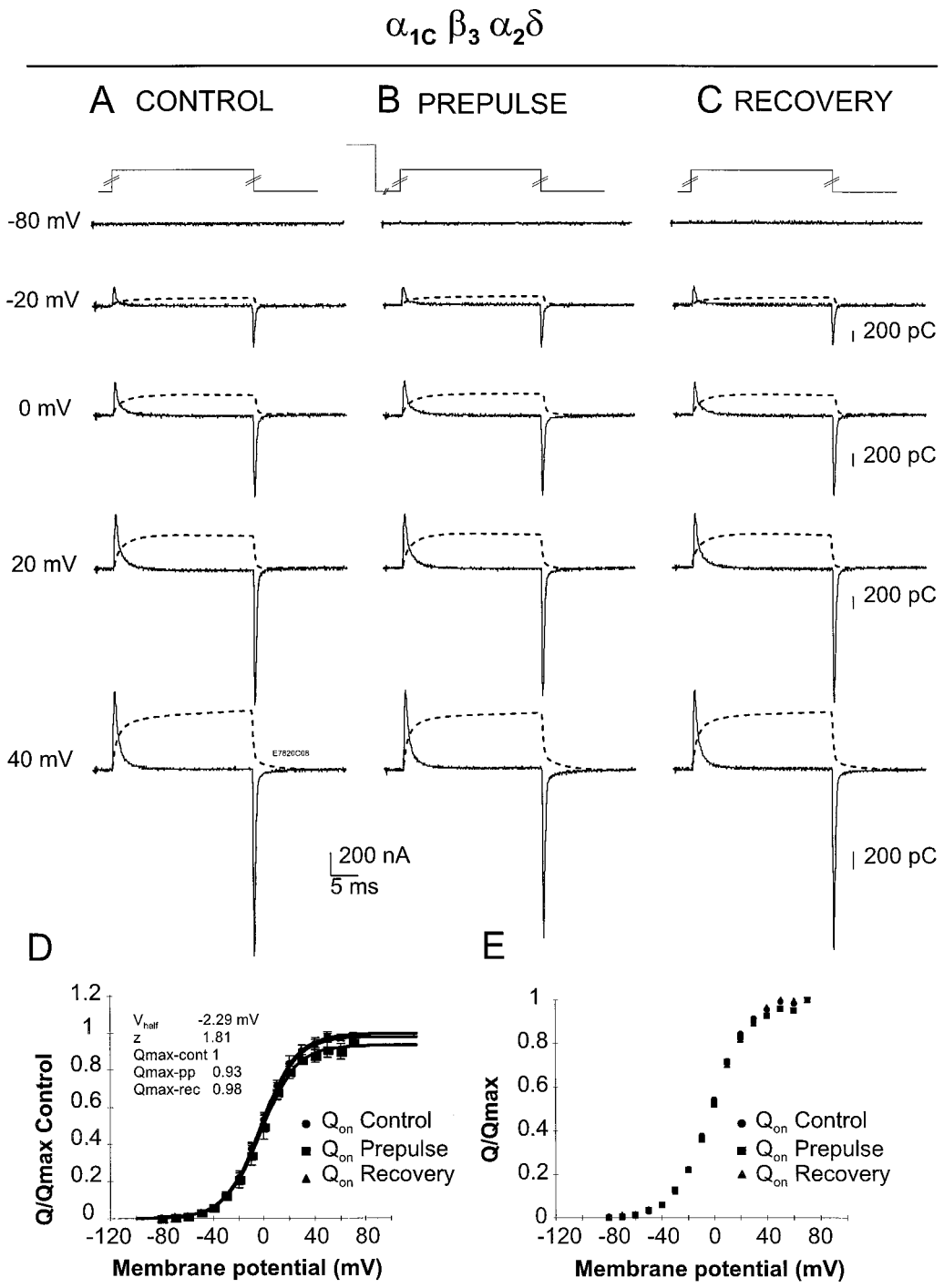

FIGURE 9 Gating currents do not potentiate in the presence of the $\alpha_2\delta$ subunit. Representative traces of gating currents from an oocyte expressing α_{1C} + β_3 + $\alpha_2\delta$ are shown. Gating currents were recorded in external 2 mM Co^{2+} and 0.2 mM La^{3+} during 30-ms depolarization to the indicated potentials. (*A*) Gating currents recorded in the absence of a positive prepulse. In (*B*) the depolarizing steps were preceded by a 200-ms prepulse to +80 mV with a time of repolarization of 50 ms between the prepulse and the test pulse. (*C*) Same conditions as in (*A*); the protocol for the recovery was run 2 min after the prepulse experiment. The dashed lines are the time integral of the gating current. (*D*) Averaged *Q-V* curves (Q_{ON}) obtained from gating currents recorded in control conditions (■), after a 200-ms prepulse to +80 mV (●), and after the recovery from potentiation (▲) (n = 4). Error bars represent SEM. Solid lines are the simultaneous fits to a single Boltzmann distribution, and the parameters used for the fitting are shown (*E*). Normalized *Q-V* curves (same as in *D*): control (●), prepulse (■), and recovery (▲).

very positive potentials (i.e., +180 mV) during the 25-ms test pulse itself. Then, the more positive part of the *G-V* curve (without prepulse) may be steeper because of the facilitation that develops during the positive pulses, thereby producing the shift.

The *G-V* curves were obtained from tail currents, which were completely abolished by replacing the external 10 mM Ba^{2+} with 2 mM Co^{2+} and 0.2 mM La^{3+}. However, although the outward current was reduced by Co^{2+} and La^{3+}, it was not completely blocked, possibly because of both the release of the block by the depolarizations and the outward ionic flux. The block of the current was restored instantaneously by membrane repolarization, as suggested by the lack of tail currents (data not shown, previously discussed in Olcese et al., 1996). Although the outward current is mainly carried by the expressed Ca^{2+} channels (it is strictly dependent on the level of Ca^{2+} channel expression and displays kinetics that depend on the subunit compositions of the expressed channel), at extreme positive potentials it could be contaminated by a small endogenous current.

Because $\alpha_2\delta$ enhances the voltage-dependent inactivation, it is reasonable to consider that the absence of facilitation in the presence of the $\alpha_2\delta$ subunit may be due to a counteracting effect on the facilitation. However, if this were the case, the two processes, facilitation and inactivation, should develop and recover with identical time courses but opposite amplitudes, exactly canceling each other out, to generate a result as the one shown in Fig. 2 *F*. Although this situation is possible, we consider it very improbable. Also, as indicated by the tail envelope test for pulses to 80 mV of increasing duration (from 25 to 200 ms) performed in the same batch of oocytes, facilitation of $\alpha_{1C} + \beta_3$ and inactivation of $\alpha_{1C} + \beta_3 + \alpha_2\delta$ develop with different time constants and relative amplitudes (data not shown). Furthermore, even though the degree of inactivation varies among batches of oocytes, we never detected facilitation in $\alpha 2\delta$-expressing oocytes even when inactivation was practically absent during the 200-ms prepulse.

Increase of charge displacement during potentiation

In $\alpha_{1C} + \beta_3$, the amount of movable charge increased after prepulses, suggesting a recruitment of a fraction of channels that are normally unable to gate during moderate depolarizations. Instead, as it was the case for the ionic current, also the charge potentiation was absent when $\alpha_2\delta$ subunits were coexpressed. We were unable to estimate the amount of the ionic current facilitation deriving from a change in gating mode and the fraction from the recruitment of new channels. It is possible that the fraction of charge facilitated by the prepulse is totally uncoupled to the channel opening. In fact, if the facilitation were produced only by newly recruited channels, it would generate an activation curve (*G-V*) with the same voltage dependence and higher limiting conductance. Instead, the left shift of the *G-V* curve associated with the kinetics changes of facilitated channels suggests a modification of the activation pathway. Nevertheless, the new channels recruited by the prepulse may contribute to the overall potentiation.

The study of the effect of prepulse facilitation on gating current can be complicated by the change in voltage dependence of the charge movement occurring in inactivated channels. As in other voltage-dependent ion channels, slow inactivation produces a shift to the left on the voltage axis of the *Q-V* curve in L-type Ca^{2+} channels. However, the shift to more negative potentials, as described by Shirokov end collaborators (1998), is produced by long depolarizations, and is further increased by coexpression of the $\alpha 2\delta$ subunit. The prepulses used in this study are short (200 ms), and no changes in the voltage dependence of the *Q-V* curves were detected after the prepulse (Figs. 8 *E* and Fig. 9 *E*).

It has been previously shown that the voltage-dependent facilitation of L-type Ca^{2+} channels is dependent on the type of β subunit coexpressed (Cens et al., 1996). Here we have shown that strong depolarizations facilitate both charge movement and ionic current in $\alpha_{1C} + \beta_3$. Thus, voltage-dependent facilitation must increase both the number of channels that are able to produce gating current and the number of channels that can open in a normal voltage range. We have also shown the involvement of the $\alpha_2\delta$ subunit in the facilitation, and its effect on ionic and gating current. A direct interaction between the $\alpha_2\delta$ and β subunits is rather unlikely, as only five amino acids of the $\alpha_2\delta$ subunit are intracellular, while the entire β subunit is known to be intracellular. The modulation exerted by the $\alpha_2\delta$ subunit on α_{1C} could instead result from a direct interaction with the pore forming subunit (Gurnett et al., 1996).

This work was supported in part by National Institutes of Health Grants AR38970 (to E.S.) and AR43411 (to L.B.), an American Heart Association grant-in-aid (to R.O.), and an American Heart Association Scientist Development grant (to N.Q.).

REFERENCES

Artalejo, C. R., D. J. Mogul, R. L. Perlman, and A. P. Fox. 1991. Three types of bovine chromaffin cell Ca^{2+} channels: facilitation increases the opening probability of a 27 pS channel. *J. Physiol.* 444:213–240.

Bangalore, R., G. Meherke, K. Gingrich, F. Hofmann, and R. S. Kass. 1996. Influence of L-type Ca channel $\alpha_2\delta$-subunit on ionic and gating current in transiently transfected HEK 293 cells. *Am. J. Physiol. Heart Circ. Physiol.* 270:H1521–H1528.

Barish, M. E. 1983. A transient calcium-dependent chloride current in the immature *Xenopus* oocyte. *J. Physiol.* 342:309–325.

Bean, B. P. 1989. Neurotransmitter inhibition of neuronal calcium currents by changes in channel voltage-dependence. *Nature.* 340:153–156.

Birnbaumer, L., K. P. Campbell, W. A. Catterall, M. M. Harpold, F. Hofmann, W. A. Horne, Y. Mori, A. Schwartz, T. P. Snutch, T. Tanabe, and R. W. Tsien. 1994. The naming of voltage-gated calcium channels. *Neuron.* 13:505–506.

Bourinet, E., P. Charnet, W. J. Tomlinson, A. Stea, T. P. Snutch, and J. Nargeot. 1994. Voltage-dependent facilitation of a neuronal alpha1C L-type calcium channel. *EMBO J.* 13:5032–5033.

Cens, T., E. M. Mangoni, S. Richard, J. Nargeot, and P. Charnet. 1996. Coexpression of the β_2 subunit does not induce voltage-dependent facilitation of the class C L-type Ca channel. *Pflugers Archiv. Eur. J. Physiol.* 431:771–774.

Cens, T., S. Restituito, A. Vallentin, and P. Charnet. 1998. Promotion and inhibition of L-type Ca^{2+} channel facilitation by distinct domains of the subunit. *J. Biol. Chem.* 273:18308–18315.

Cloues, R. K., S. J. Tavalin, and N. V. Marrion. 1997. Beta-adrenergic stimulation selectively inhibits long-lasting L-type calcium channel facilitation in hippocampal pyramidal neurons. *J. Neurosci.* 1:17: 6493–6503.

Costantin, J. L., N. Qin, J. Zhou, D. Platano, L. Birnbaumer, and E. Stefani. 1998. Long lasting facilitation of the rabbit cardiac Ca^{2+} channel: correlation with the coupling efficiency between charge movement and pore opening. *FEBS Lett.* 423:213–217.

Dai, S., N. Klugbauer, X. Zong, C. Seisenberger, and F. Hofmann. 1999. The role of subunit composition on prepulse facilitation of the cardiac L-type calcium channel. *FEBS Lett.* 442:70–74.

Dolphin, A. C. 1996. Facilitation of Ca^{2+} current in excitable cells. *TINS.* 19:35–43.

Fedida, D., D. Noble, and A. J. Spindler. 1988. Mechanism of the use dependence of the calcium current in guinea pig myocytes. *J. Physiol.* 405:461–475.

Felix, R., C. A. Gurnett, M. De Waard, and K. P. Campbell. 1997. Dissection of functional domains of the voltage-dependent Ca^{2+} channel $\alpha_2\delta$ subunit. *J. Neurosci.* 17:6884–6891.

Gurnett, A. C., M. De Waart, and K. P. Campbell. 1996. Dual function of the voltage-dependent Ca^{2+} channel $\alpha_2\delta$ subunit in current stimulation and subunit interaction. *Neuron.* 16:431–440.

Ikeda, S. R. 1996. Voltage-dependent modulation of N-type calcium channels by G-protein $\beta\gamma$ subunits. *Nature.* 380:255–258.

Johnson, B., D. T. Scheuer, and W. A. Catterall. 1994. Voltage-dependent potentiation of L-type Ca^{2+} channels in skeletal muscle cells requires anchored cAMP-dependent protein kinase. *Proc. Natl. Acad. Sci. USA.* 91:11492–11496.

Kavalali, E. T., and M. R. Plummer. 1996. Multiple voltage dependent mechanisms potentiate calcium channel activity in hippocampal neurons. *J. Neurosci.* 16:1072–1082.

Lee, K. S. 1987. Potentiation of the calcium channel currents of internally perfused mammalian heart cell by repetitive depolarizations. *Proc. Natl. Acad. Sci. USA.* 84:3941–3945.

Neely, A., X. Wei, R. Olcese, L. Birnbaumer, and E. Stefani. 1993. Potentiation by the β subunit of the ratio of the ionic current to the charge movement in the cardiac calcium channel. *Science.* 262:575–578.

Neely, A., R. Olcese, X. Wei, L. Birnbaumer, and E. Stefani. 1994. Ca^{2+}-dependent inactivation of a cloned cardiac Ca^{2+} channel alpha 1 subunit (α_{1C}) expressed in *Xenopus* oocytes. *Biophys. J.* 66:895–1903.

Noble, S., and T. Shimoni. 1981a. The calcium and frequency dependence of the slow inward current "staircase" in frog atrium. *J. Physiol.* 310: 57–75.

Noble, S., and T. Shimoni. 1981b. Voltage dependent potentiation of the slow inward current in frog atrium. *J. Physiol.* 310:77–95.

Olcese, R., A. Neely, N. Qin, X. Wei, L. Birnbaumer, and E. Stefani. 1996. Coupling between charge movement and pore opening in type-E Ca^{2+} channel. *J. Physiol.* 497:675–686.

Olcese, R., N. Qin, T. Schneider, A. Neely, X. Wei, E. Stefani, and L. Birnbaumer. 1994. The amino terminus of a calcium channel beta subunit sets rates of channel inactivation independently of the subunit's effect on activation. *Neuron.* 13:1433–1438.

Perez-Reyes, E., A. Castellano, H. S. Kim, P. Bertrand, E. Baggstrom, A. E. Lacerda, X. Wei, and L. Birnbaumer. 1992. Cloning and expression of cardiac/brain β subunit of the L-type calcium channel. *J. Biol. Chem.* 267:1792–1797.

Pietrobon, D., and P. Hess. 1990. Novel mechanism of voltage dependent gating in L-type calcium channel. *Nature.* 346:651–655.

Platano, D., N. Qin, F. Noceti, L. Birnbaumer, E. Stefani, and R. Olcese. 1998. Increase of charge movement during prepulse facilitation in L-type Ca^{2+} channels and modulatory effect of $\alpha_2\delta$ subunit. *Biophys. J.* 74:102*a*. (Abstr.).

Qin, N., R. Olcese, E. Stefani, and L. Birnbaumer. 1998a. Modulation of human neuronal α_{1E}-type calcium channel by the $\alpha_2\delta$ subunit. *Am. J. Physiol. Cell Physiol.* 274:C1324–C1331.

Qin, N., D. Platano, R. Olcese, J. L. Costantin, E. Stefani, and L. Birnbaumer. 1998b. Unique regulatory properties of type 2a Ca2+ channel β subunit due to palmitoylation. *Proc. Natl. Acad. Sci. U.S.A.* 95: 4690–4695.

Qin, N., D. Platano, R. Olcese, E. Stefani, and L. Birnbaumer. 1997. Direct interaction of G$\beta\gamma$ with a novel C-terminal G$\beta\gamma$ binding domain of α1 is responsible for inhibition of presynaptic Ca^{2+} channels by G-protein-coupled receptors *Proc. Natl. Acad. Sci. U.S.A.* 94:8866–8871.

Rakowski, R. F. 1993. Charge movement by the Na/K pump in *Xenopus* oocytes. *J. Gen. Physiol.* 101:117–144.

Sanford, J., J. Codina, and L. Birnbaumer. 1991. Gamma-subunits of G proteins, but not their alpha- or beta-subunits, are polyisoprenylated. Studies on post-translational modifications using in vitro translation with rabbit reticulocyte lysates. *J. Biol. Chem.* 266:9570–9579.

Shirokov, R., G. Ferreira, J. Yi, and E. Rios. 1998. Inactivation of gating currents of L-type calcium channels. Specific role of the $\alpha_2\delta$ subunit. *J. Gen. Physiol.* 111:807–823.

Singer-Lahat, D., I. Lotan, M. Biel, V. Flockerzi, F. Hofmann, and F. Dascal. 1994. Cardiac calcium channels expressed in Xenopus oocytes are modulated by dephosphorylation but not by cAMP-dependent phosphorylation. *Receptors and Channels.* 2:215–226.

Stefani, E., and F. Bezanilla. 1998. The cut open oocyte voltage clamp technique. *Methods Enzymol.* 293:300–318.

Wei, X., A. Neely, R. Olcese, W. Lang, E. Stefani, and L. Birnbaumer. 1996. Increase in Ca^{2+} channel expression by deletions at the amino terminus of the cardiac α_1 subunit. *Receptors and Channels.* 4:205–215.

Wei, X. Y., E. Perez-Reyes, A. E. Lacerda, G. Schuster, A. M. Brown, and L. Birnbaumer. 1991. Heterologous regulation of the cardiac Ca^{2+} channel α_1 subunit by skeletal muscle β and γ subunits. Implication for the structure of cardiac L-type Ca^{2+} channels *J. Biol. Chem.* 266: 21943–21947.

Zygmunt, A. C., and J. Maylie. 1990. Stimulation-dependent facilitation of the high threshold calcium current in guinea-pig ventricular myocytes. *J. Physiol.* 428:653–671.